Earthquake Geotechnical Engineering for Protection and Development of Environment and Constructions – Silvestri & Moraci (Eds)
 ISBN 978-0-367-14328-2

On small strain shear stiffness of plastic clay subjected to isotropic stress states

M. Khoshini, L. Zhang & A. Khoshghalb
School of Civil and Environmental Engineering, UNSW Sydney, Sydney, Australia

M. Payan
Faculty of Civil Engineering, Khajeh Nasir Toosi University of Technology, Tehran, Iran.

ABSTRACT: It is generally established that the state of stress, void ratio and over-consolidation ratio are the key parameters influencing the small strain stiffness of clays. Many semi-empirical expressions have been introduced to evaluate this important parameter using different approaches. In this study, a set of bender elements experiments along isotropic loading and unloading stress paths are performed on a saturated typical plastic clay sample. The clay sample is carefully reconstituted in the laboratory using the static compaction technique to a target density. The sample is then saturated and tested under several loading-unloading isotropic stress paths using a stress-path triaxial apparatus equipped with a pair of bender elements on the base pedestal and top cap. Exploiting the results of the experiments, a discussion is made on the validity of the current approaches in the literature in estimating the small-strain shear modulus of clays, particularly in capturing the effects of the void ratio.

1 INTRODUCTION

Dynamic properties of soils are important parameters in the design of geo-structures subjected to static and dynamic loading. These properties enable engineers to conduct appropriate analyses and form reliable predictions about ground motions and structural deformation (Clayton, 2011). One of the key parameters for dynamic analysis of geo-structures is the small strain shear modulus, typically denoted by G_{max}. Many geotechnical problems such as deformations in embankments, foundation stability and dynamic soil-structure interactions rely on the accurate estimation of the small strain shear modulus of soils.

There have been numerous studies in the literature on the small-strain shear modulus of granular materials including Hardin and Richart (1963), Saxena et al. (1988), Menq (2003), Wichtmann and Triantafyllidis (2009), Payan et al. (2016a), and Payan et al. (2016b), to name a few. On the contrary, there exist much fewer studies throughout the literature associated with the small-strain dynamic properties of clayey soils (Viggiani and Atkinson, 1995, Shibuya et al., 1998, Rampello et al., 1997, Clayton and Heymann, 2001, Subramaniam and Banerjee, 2016), mainly due to the difficulties in testing plastic clays under drained conditions. Clayey soils are commonly encountered in civil engineering constructions like embankments, dams, dykes, levees, and liners. In order to design and construct safer infrastructures, extensive and reliable investigation on dynamic properties of saturated clays under different loading conditions is necessary, especially at small strain range.

In a pioneer study performed by Hardin and Richart (1963), the small-strain shear modulus of clay was correlated to a function of void ratio, $f(e)$, over-consolidation ratio, OCR, and mean effective stress, p':

$$G_{max} = A.f(e).OCR^k.\left(\frac{p'}{p_a}\right)^n \tag{1}$$

where p_a is the atmospheric pressure and *A, n* and *k* are fitting parameters which are dependent on the properties of the soil of interest. According to Hardin and Richart (1963) and Hardin and Black (1968), under isotropic conditions, soil behaviour depends on both the current stress state and history of stress.

Equation (1) is general considering all clay types. According to the critical state soil mechanics framework, to capture the state of a particular clay under isotropic pressure, only two state parameters are required (Schofield and Wroth, 1968, Viggiani and Atkinson, 1995). The choice of the state parameters is immaterial and is only a matter of convenience and practicality. The current effective stress has been unanimously adopted in the literature as one of the state parameters, however, for the selection of the second state variable, two major approaches have been formed among the researchers to estimate the small strain shear modulus of clay under isotropic loading conditions. Some researchers (e.g. Viggiani and Atkinson (1995) and Rampello et al. (1997)), have adopted the over-consolidation ratio, *OCR*, to investigate G_{max} of clayey soils, while others (e.g., Hardin and Black, 1968, Marcuson and Wahls, 1972, Jamiolkowski et al., 1991, Shibuya et al., 1998, Clayton and Heymann, 2001) have used the void ratio, *e*, for the same purpose. Somewhat surprisingly, the latter group has often assumed void ratio functions which are very similar to or exactly the same as those obtained for granular soils. This is, perhaps, partly due to the original recommendation by Hardin and Richart (1963). Furthermore, difficulties in testing saturated clays in drained condition and their wide range of characteristics and behaviours have been preventive in the generation of a large experimental data sets so that appropriate void ratio functions for clays can be developed. Despite the original recommendation by Hardin and Richart (1963) which has been subsequently adopted by several researchers (e.g., Marcuson and Wahls (1972) and Kim and Novak (1981)), there is no evidence to allude that the void ratio dependencies of G_{max} in clays and sands are the same, due to their vastly different structures and characteristics.

In the present study, a set of bender element tests are carefully performed on a sample of a plastic clay along isotropic loading and unloading stress paths. Utilizing the results of these tests, the small-strain shear modulus of the clay sample at variable void ratios, over-consolidation ratios and mean effective stresses are measured. Accordingly, the variations of G_{max} with *e, OCR*, and *p'* are investigated in order to evaluate the suitability of the common void ratio functions in capturing the effect of the state of the clay on its G_{max}.

2 TEST MATERIAL AND EXPERIMENTAL APPROACH

2.1 *Test materials*

The clay sample used in this study is the Shellharbour clay from the Illawarra region, NSW, Australia. The Atterberg limits and particle specific gravity of the clay are summarized in Table 1. The Shellharbour clay is classified as ML according to the Unified Soil Classification System (USCS).

Table 1. Index properties of the tested clay

Soil Name	*LL (%)*	*PL (%)*	*PI (%)*	G_s	USCS Classification
Shellharbour clay	42	31	11	2.75	ML

2.2 *Sample preparation*

For sample preparation, the soil was oven dried at 105°C for at least 24 hours to reach a dry state. The clay crumbs were then crushed and sieved through sieve No.75 (425 μm) to remove the coarse-grained particles. The slurry consolidation method was adopted herein for sample preparation. The sieved material was mixed with de-aired water to obtain a homogeneous slurry with a water content 1.85 times the liquid limit of the clay. The slurry was then poured into a cylindrical mould and consolidated for around two weeks to reach the target void ratio.

2.3 *Testing procedure and experimental program*

The prepared soil sample was carefully put into an expanded membrane and then positioned carefully on the base pedestal of a stress-path triaxial apparatus equipped with bender elements (Figure 1).

The sample was saturated using the escalated back pressure and cell pressure method until a B-value larger than 0.95 was achieved. The saturated sample was then subjected to several isotropic loading and unloading steps. Initially, a 10 kPa mean effective stress, was applied to the sample followed by p' of 40, 75, and 100 kPa. The sample was then unloaded to 10 kPa at the same stress intervals. Another loading stage was then taken to re-load the sample to 150, 300, and 450 kPa mean effective stresses, followed by the second step-by-step unloading process down to 10 kPa. The volume change of the sample was precisely captured in all the loading and unloading steps by measuring the amount of water entering or exiting the sample. The testing procedure followed forced the clay sample to pass through various void ratios (e), mean effective stresses (p') and over-consolidation ratios (OCR) as presented in Table 2.

The bender element test was performed at each stage of loading and unloading to obtain the shear wave velocity in the clay, and therefore the small strain shear modulus of the clay at various stress states along the adopted stress path. At each stress state and prior to the bender element test, adequate time was given to the sample to make sure that the fully drained condition has reached and all the excess pore water pressure has been dissipated. Knowing the volumetric strain of the sample, the void ratio at each stress state was calculated. The void ratio evolution during the loading and unloading process versus the mean effective stress is plotted in Figure 2.

From the bender element test results, the velocity of the shear stress wave through the soil medium (V_s) was measured using the tip-to-tip distance through the clay specimen (L_{eff}) and the time required for the shear stress wave generated at the transmitter bender element to

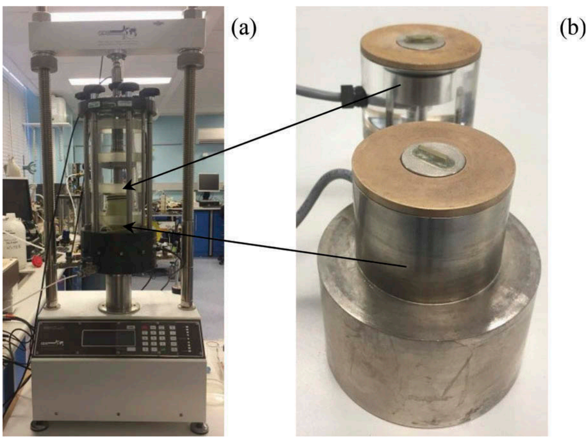

Figure 1. The stress-path triaxial apparatus (a) equipped with top-cap and pedestal bender elements (b) used in this study

Table 2. state parameters at each test point along the stress path

p' (kPa)	10	40	75	100	75	50	25	10	150	300	450	300	150	100	50	25	10
OCR	7.5	1.9	1	1	1.3	2	4	10	1	1	1	1.5	3	4.5	9	18	45
e	1.28	1.26	1.24	1.21	1.22	1.22	1.23	1.25	1.17	1.06	0.97	0.98	0.99	0.99	1.00	1.01	1.03

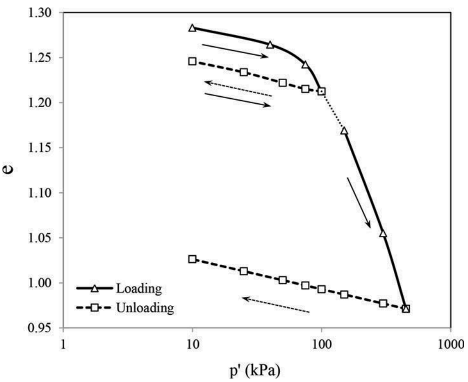

Figure 2. The variation of void ratio with mean effective stress along the stress path adopted.

reach the receiver bender element (t). Thereafter, the small strain shear modulus of the clay specimen was calculated as

$$V_s = \frac{L_{eff}}{t} \tag{2}$$

$$G_{max} = \rho V_s^2 \tag{3}$$

where ρ is the density of the clay sample. It is worth noting that in order to measure the shear wave velocity, both the first-time arrival and peak-to-peak interpretations were attempted in this study. The results of the two approaches were very similar in all cases. Therefore, the first time arrival approach was adopted consistently to obtain the small strain shear modulus of the sample. The recorded G_{max} data points along loading and unloading stress paths are plotted against the normalized mean effective stress and void ratio in Figure 3.

3 RESULTS AND DISCUSSION

3.1 *Evaluation of the current void ratio functions*

The test data is analyzed in this section to see how well the void ratio functions often adopted in the literature can capture the effect of clay density on its small strain shear modulus. Accordingly, the following equation is often adopted for the estimation of the small strain shear modulus of a clay,

$$G_{max} = A.f(e).\left(\frac{p'}{p_a}\right)^n \tag{4}$$

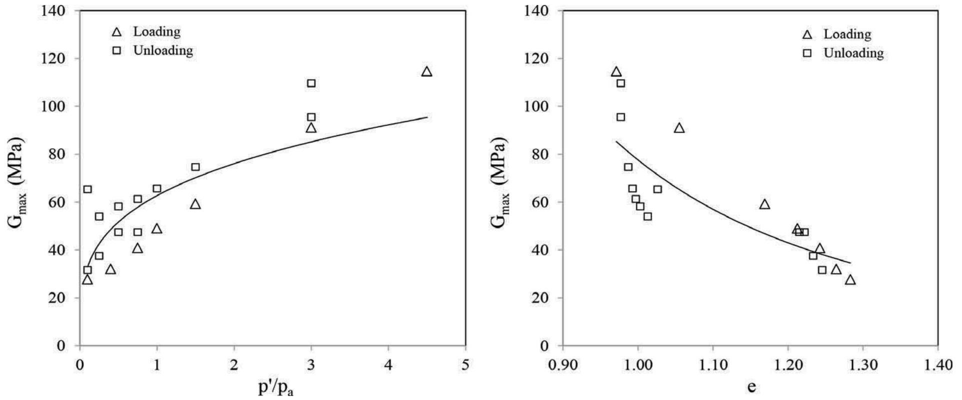

Figure 3. G_{max} data as a function of normalized mean effective stress and void ratio along both loading and unloading stress paths.

where A and n are fitting parameters to be determined experimentally, and $f(e)$ is a void ratio function to capture the effect of clay density on its G_{max}. There are two major forms of void ratio functions for clays in the literature. One function is based on the suggestion of Hardin and Black (1968) with the form of $f_1(e) = (a - e)^2/1 + e$ with $a = 2.973$ (Hardin and Black, 1968, Kim and Novak, 1981), $a = 4.4$ (Marcuson and Wahls, 1972), and $a = 7.32$ (Kokusho et al., 1982). The other void ratio functions are power form of $f_2(e) = e^{-1.3}$ (Jamiolkowski et al., 1991, Payan et al., 2016a) and $f_3(e) = (1 + e)^{-2.4}$ (Shibuya et al., 1998).

To see how well these void ratio functions perform, the parameters A and n are obtained for each of the void ratio functions (referred to as A_i and n_i when $f_i(e)$ is used) based on the experimental results of the normally consolidated clay of this study (OCR=1). To this end, the small strain shear modulus values for data points with OCR=1 normalized against void ratio functions, are plotted against the normalized mean effective stress, as shown in Figures 4-a,c, e,g, and i. Using the best-fit power-type law, the parameters A and n were found in each case as shown on the corresponding graph in Figure 4.

Having obtained parameters A and n, the small strain shear modulus of the clay can now be predicted using $G_{max\text{-}predicted} = A\, f(e)\, (p'/p_a)^n$. If the G_{max} dependency to the state of the clay is properly captured by this equation, one would expect that the equation can be equally applied to over-consolidated samples of the same clay too, and that if the measured

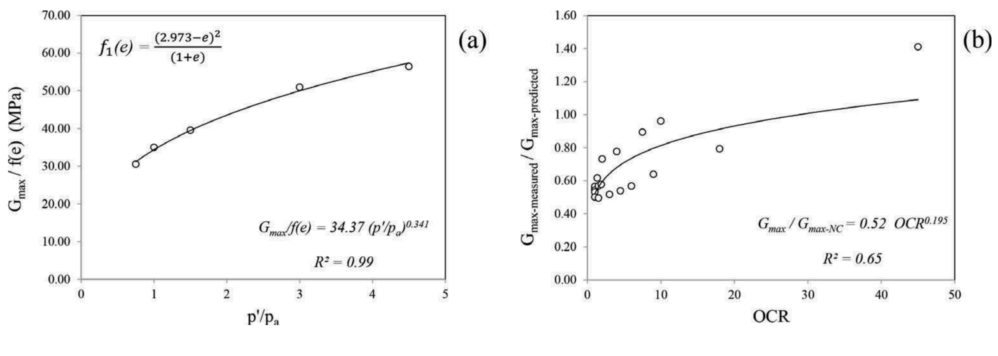

Figure 4. (a), (c), (e), (g), and (i): variations of the normalized small strain shear modulus against different void ratio functions with normalized mean effective stress for normally consolidated states of the sample (OCR=1); (b), (d), (f), (h), and (j): variations of the measured small strain shear modulus normalized against the predicted small strain shear modulus (using different mean effective stress and void ratio functions) with over-consolidation ratio

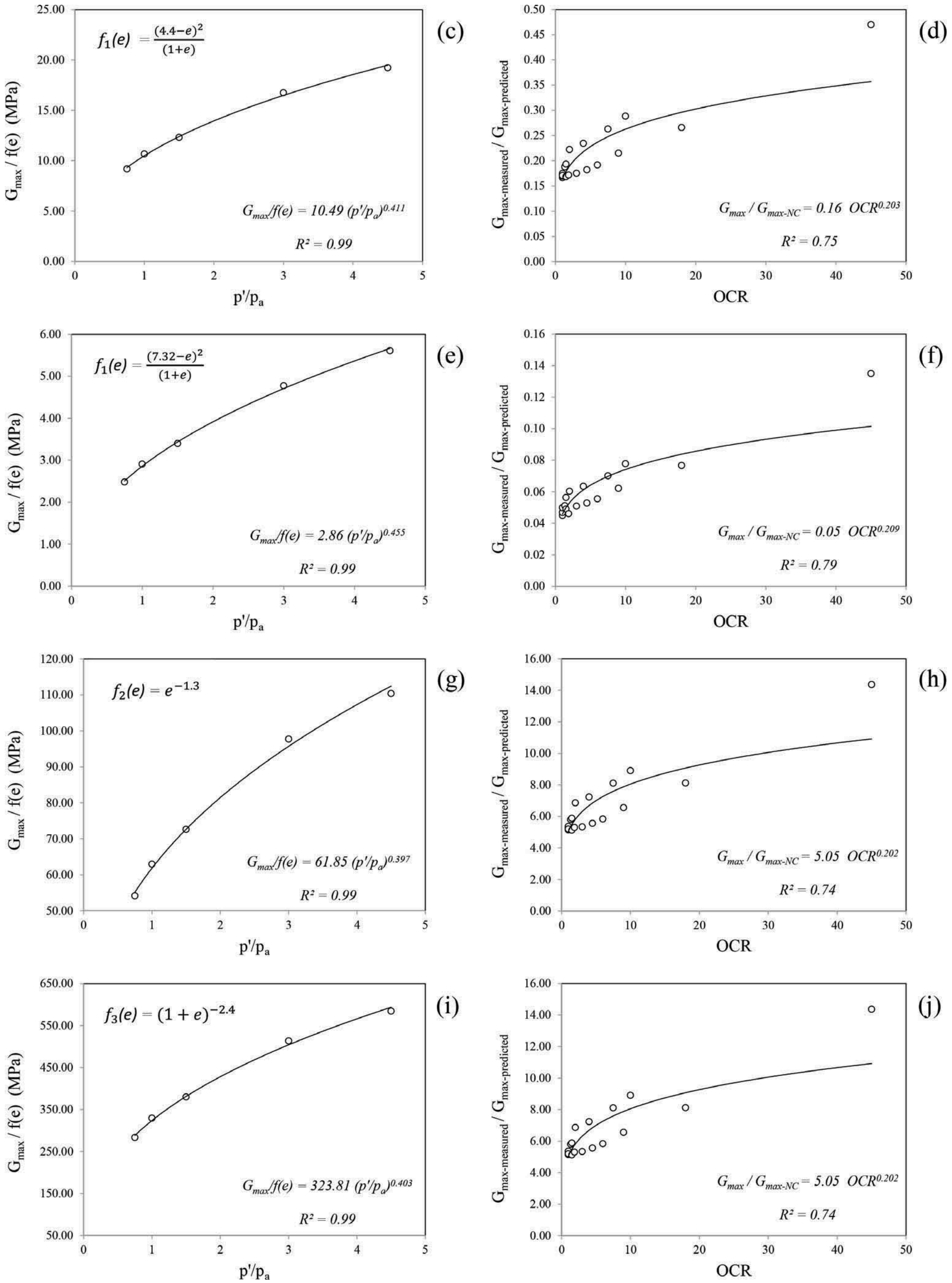

Figure 4. (*continued*)

G_{max} values are normalized against the predicted small strain shear modulus $G_{max\text{-}predicted} = A\, f(e)(p'/p_a)^n$, no discernible trend is observed with the *OCR*. Such normalization has been performed for all the data points, and the results are plotted against *OCR* in Figures 4-b,d,f, h, and j. As illustrated in this figure, $G_{max\text{-}measured}/G_{max\text{-}predicted}$ has an obvious trend with *OCR* for every void ratio function used. It suggests that neither of the void ratio functions would result in a relationship capable of fully capturing the effect of the state of the sample on its G_{max}.

3.2 *Implementation of the over-consolidation ratio instead of the void ratio*

As mentioned previously and according to the critical state soil mechanics, it should be possible to capture the effect of the clay state on its small strain shear modulus using p' and the *OCR* instead of p' and the void ratio. To this end, the G_{max} of the clay is evaluated as,

$$G_{max} = B\left(\frac{p'}{p_a}\right)^m OCR^k \tag{5}$$

The parameters *B, m* and *k* are again fitting parameters and have to be obtained from the experimental data. Compared to the previous case, there is one more parameter in this approach. The reason is that there is no presumption for the variation of G_{max} with *OCR*, mainly because *OCR* is not often used in the description of granular materials, and therefore there is no relevant relation for granular materials to be adopted for clays in a similar way that has been done for void ratio functions. Although on the surface, this increases the experimental efforts required for parameter identification, it indeed avoids the problems highlighted in the previous section, as the model parameters are often identified individually in this approach, and the G_{max} model is developed with no presupposition. This procedure is now explained for the data of this study.

First parameters *B* and *m* are obtained by plotting the G_{max} of the normally consolidated samples against the normalized mean effective stress (Figure 5-a). For the data of this study, this results in B=48.16 MPa and m=0.575. Now, test data with $OCR>1$ are used to obtain the OCR dependency of the G_{max}. To this end, measured G_{max} values are normalized against $G_{max\text{-}NC} = B(p'/p_a)^m$ and plotted against *OCR*, as seen in Figure 5-b. This results in k=0.366 for the data of this study.

Equation (5) can now be tested to see if it properly captures the effect of state parameters on G_{max} or not, using an argument and procedure similar to that adopted in the previous section: If the proposed equation captures the state of the soil properly, when the measured G_{max} values are normalized against the predicted ones, no discernible trend is expected against any other state variable like void ratio. Figure 6 shows the variation of $G_{max\text{-}measured}/G_{max\text{-}predicted}$ against the void ratio. As can be seen from this figure, while there are some scatters in the data which is unavoidable in any empirical model for G_{max}, and any experimental work, no

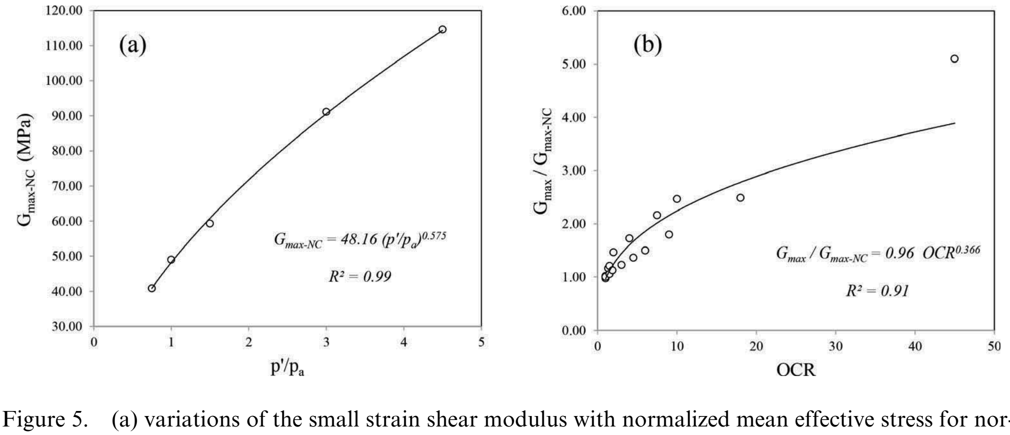

Figure 5. (a) variations of the small strain shear modulus with normalized mean effective stress for normally consolidated clay samples (*OCR*=1); (b) variations of the normalized small strain shear modulus against small strain shear modulus developed for normally consolidated clays, with the over-consolidation ratio

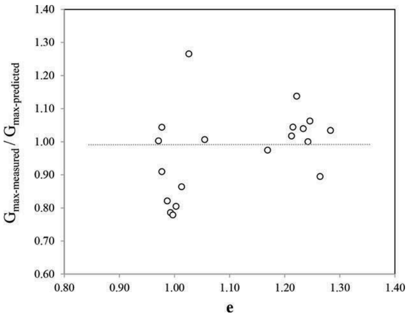

Figure 6. Variation of the measured small strain shear modulus normalized against the predicted small strain shear modulus (using mean effective stress and over-consolidation ratio) with the void ratio.

detectable trend could be observed in the data points. This indicates that the procedure followed has successfully captured the effect of the soil state on its G_{max}, and has resulted in an appropriate relationship for estimation of the small strain shear modulus of the clay of interest.

It has to be emphasized that this relationship is only valid for the specific clay studied in this research, and the model parameters need to be recalibrated for other types of clay using the procedure explained.

4 CONCLUSION

In this study, the small strain shear modulus of a clayey soil was investigated on several isotropic loading-unloading paths. The variation of the sample void ratio was monitored along the loading-unloading path using the amount of water expelled from the saturated clay specimen. At the end of each equilibrium stage, the velocity of the shear wave passing through the sample was measured using the bender element test, and the small strain shear modulus was accordingly obtained. The influence of the three major parameters (i. e. the mean effective stress, void ratio and over-consolidation ratio) on the small strain shear modulus of the clay sample was investigated.

It was shown that the commonly used void ratio functions for clays are not fully capable of secluding the effect of *OCR* on the small strain shear modulus of the sample, and therefore incapable of fully capturing the state of the clay. On the other hand, the power function for *OCR* was successful in capturing the state of the sample due to the independent identification of the power parameter involved. In theory, similar independent parameter identification can be performed with a void ratio function too, but this is rarely the case in the literature.

Finally, it has to be noted that the best fit values presented in this study for model parameters are obtained only for the specific clay tested, and based on a limited number of data points, so they have no specific importance. The main goal of the study was to show that adoption of the void ratio functions developed for granular materials for clays, which is widespread in the literature, is in general erroneous.

REFERENCES

Clayton, C. & Heymann, G. 2001. Stiffness of geomaterials at very small strains. *Géotechnique*, 51, 245–255.

Clayton, C. 2011. Stiffness at small strain: research and practice. *Géotechnique*, 61, 5–37.

Hardin, B. O. & Richart, J. F. 1963. Elastic wave velocities in granular soils. *Journal of Soil Mechanics & Foundations Div*, 89.

Hardin, B. O. & Black, W. L. 1968. Vibration modulus of normally consolidated clay. *Journal of Soil Mechanics & Foundations Div*.
Jamiolkowski, M., Leroueil, S. & Lo Presti, D. C. Design parameters from theory to practice. Int. Conf. on Geotechnical Engineering for coastal development, 1991. Port & Harbour Research Institute, 877–917.
Kim, T. & Novak, M. 1981. Dynamic properties of some cohesive soils of Ontario. *Canadian Geotechnical Journal*, 18, 371–389.
Kokusho, T., Yoshida, Y. & Esashi, Y. 1982. Dynamic properties of soft clay for wide strain range. *Soils and Foundations*, 22, 1–18.
Marcuson, W. F. & Wahls, H. E. 1972. Time effects on dynamic shear modulus of clays. *Journal of Soil Mechanics & Foundations Div*, 98.
Menq, F. Y. 2003. Dynamic properties of sandy and gravelly soils. PhD dissertation, University of Texas at Austin, USA.
Payan, M., Khoshghalb, A., Senetakis, K. & Khalili, N. 2016a. Effect of particle shape and validity of Gmax models for sand: A critical review and a new expression. *Computers and Geotechnics*, 72, 28–41.
Payan, M., Senetakis, K., Khoshghalb, A. & Khalili, N. 2016b. Effect of gradation and particle shape on small-strain Young's modulus and Poisson's ratio of sands. *International Journal of Geomechanics*, 17, 04016120.
Rampello, S., Viggiani, G. & Amorosi, A. 1997. Small-strain stiffness of reconstituted clay compressed along constant triaxial effective stress ratio paths. *Géotechnique*, 47, 475–489.
Saxena, S. K., Avramidis, A. S. & Reddy, K. R. 1988. Dynamic moduli and damping ratios for cemented sands at low strains. *Canadian Geotechnical Journal*, 25, 353–368.
Schofield, A. & Wroth, P. 1968. *Critical state soil mechanics*, McGraw-Hill London.
Shibuya, S., Hwang, S. & Mitachi, T. 1998. Elastic shear modulus of soft clays from shear wave velocity measurement. *Pre-failure deformation behaviour of geomaterials*, 207.
Subramaniam, P. & Banerjee, S. 2016. Torsional Shear and Resonant Column Tests on Cement Treated Marine Clay. *Indian Geotechnical Journal*, 46, 183–191.
Viggiani, G. & Atkinson, J. 1995. Stiffness of fine-grained soil at very small strains. *Géotechnique*, 45, 249–265.
Wichtmann, T. & Triantafyllidis, T. 2009. Influence of the grain-size distribution curve of quartz sand on the small strain shear modulus G max. *Journal of geotechnical and geoenvironmental engineering*, 135, 1404–1418.